Journal of Materials Chemistry B

Accepted Manuscript

This article can be cited before page numbers have been issued, to do this please use: S. Hamsici, G. Cinar, A. Celebioglu, T. Uyar, A. B. Tekinay and M. O. Guler, *J. Mater. Chem. B*, 2016, DOI: 10.1039/C6TB02441F.

ROYAL SOCIETY OF CHEMISTRY

rsc.li/materials-b

View Article Online
DOI: 10.1039/C6TB02441F

Journal of Materials Chemistry B

ARTICLE

Bioactive Peptide Functionalized Aligned Cyclodextrin Nanofibers for Neurite Outgrowth

Received 00th January 20xx,
Accepted 00th January 20xx

DOI: 10.1039/x0xx00000x

www.rsc.org/

Seren Hamsici,[a] Goksu Cinar,[a] Asli Celebioglu,[a] Tamer Uyar,[a,*] Ayse B. Tekinay,[a,*] and Mustafa O. Guler [a,*]

Guidance of neurite extension and establishment of neural connectivity hold great importance for neural tissue regeneration and neural conduit implants. Although bioactive-epitope functionalized synthetic or natural polymeric materials have been proposed for induction of neural regeneration, chemical modifications of these materials for neural differentiation still remain a challenge due to harsh conditions of chemical reactions, along with non-homogeneous surface modifications. In this study, a facile noncovalent functionalization method is shown by exploiting host-guest interactions between an adamantly-conjugated laminin derived bioactive IKVAV epitope and electrospun cyclodextrin nanofibers (CDNFs) to fabricate implantable scaffolds for peripheral nerve regeneration. While electrospun CDNFs introduce a three-dimensional biocompatible microenvironment to promote cellular viability and adhesion, the bioactive epitopes presented on the surface of electrospun CDNFs guide cellular differentiation for PC-12 cells. In addition to materials synthesis and smart functionalization, physical alignment of the electrospun nanofibers guides the cells for enhanced differentiation. Cells cultured on aligned and IKVAV functionalized electrospun CDNFs had significantly higher expression of neuron-specific βIII-tubulin and synaptophysin. The neurite extension is also higher on the bioactive aligned scaffolds compared to random and non-functionalized electrospun CDNFs. Both chemical and physical cues were utilized for an effective neuronal differentiation process.

[a] Institute of Materials Science and Nanotechnology, National Nanotechnology Research Center (UNAM), Bilkent University, Ankara 06800, Turkey
*Correspondence - moguler@unam.bilkent.edu.tr, gulermus@hotmail.com
Electronic Supplementary Information (ESI) available: LC-MS and experimental details are provided. See DOI: 10.1039/x0xx00000x

View Article Online
DOI: 10.1039/C6TB02441F

Introduction

Neurotraumas including spinal cord and peripheral nerve injuries are significant health problems across the world and cause severe disabilities with more than 100,000 new injuries each year. [1] Nerve autografts constitute the gold standard for the treatment of peripheral nerve injuries, however only half of the patients fully recover after treatment due to the problems associated with donor shortage, mismatch between donor nerve and injury site, immunological problems and the need for secondary surgeries.[2,3] These problems have led to the development of alternative medical therapies focused on biomaterials that are able to guide and direct neural cells to promote recovery of motor or sensory functions.[4,5] Biomaterials are used for the treatment of peripheral nerve injuries by repairing and regenerating damaged tissue by mimicking the native environment of neuronal cells.[6,7] Extracellular matrix (ECM) acts as a structural support and includes a wide range of polysaccharide chains and fibrous proteins that present biochemical and biomechanical cues for the proliferation, differentiation and migration of cells.[8] Therefore, the design of bioactive, ECM-mimetic scaffolds can facilitate the attachment of cells, enable nutrient transport with their porous structure and provide relevant signals to cells.[9]

Electrospinning is a widely-used fabrication technique for producing fibers ranging in diameters from nanometers to micrometers. Due to the ease of control on structural, mechanical and biological properties of the fabricated materials, electrospinning has been widely utilized for biomaterial production.[10–12] The most common polymers used in electrospinning process for nerve tissue-engineered grafts are poly(l-lactic acid) (PLLA), poly(lactic-co-glycolic-acid) (PLGA) and poly(ε-caprolactone) (PCL) due to their biodegradability and biocompatibility.[13] On the other hand, the nonbioactive and hydrophobic nature of these polymers limit cell-materials interactions, which may cause problems in the essential cellular bioprocesses for neural differentiation.[14] In order to improve hydrophilicity and bioactivity of electrospun polymeric materials, additional approaches such as chemical covalent binding,[15] air plasma treatment[16] and blending during electrospinning[17] can be performed. Furthermore, electrospun nanofibers were chemically functionalized with laminin or laminin derived epitopes to promote neural cell affinity, recovery and neurite extension. [18–20]Becker *et al.* functionalized PLLA fibers with a laminin derived epitope by click chemistry and showed the improved effect of the peptide conjugated fibers on neural cells in terms of neurite extension.[19] In another approach, Lee *et al.* applied air plasma method using ammonia gas to develop electrospun PLGA scaffolds presenting amino-rich and hydrophilic surface characteristics for cellular adhesion and proliferation.[21] However, adjusting the surface homogeneity and controlling exposure time are challenging issues since the air plasma affects only a limited depth in electrospun scaffolds.[22] In addition to chemical conjugation approaches, Ramakrishna *et al.* prepared PCL nanofibers, which were either blended with laminin or encapsulated laminin in the core of PCL nanofibers by electrospinning process.[23] However, the natural proteins could be denatured during the electrospinning process, because of the harsh conditions of organic solvents. Besides functionalization, the orientation of the electrospun fibers is another important feature for designing biomaterials for neural tissue engineering.[24,25] Uniaxially aligned fibers guide regenerating axons and induce the extension of the neurites along the direction of the scaffold, which is able to enhance repair of nerve defects even in the presence of long peripheral nerve gaps.[26–28] Supramolecular host-guest chemistry is a novel surface functionalization method due to the high specificity of recognition motifs through noncovalent interactions.[29] Cyclodextrins (CDs) are composed of glucopyranose subunits, and they are one of the most intriguing oligosaccharide types due to their ability to form noncovalent host-guest interaction complexes through their cyclic and truncated cone-shaped structures.[30–32] Due to the non-toxic and low-cost properties of CDs, which are obtained by the enzymatic degradation process of starch, they have been widely used in the pharmaceutical, food and cosmetic industries.[32,33] One of the most well-known noncovalent host-guest interactions is observed between CD and adamantane molecules, in which the CD cavity serves as a host while adamantane is a hydrophobic guest molecule.[34] Stupp *et al.* used a similar approach to attach a biofunctional adamantane conjugated bioactive peptide epitope on CD surfaces in order to enhance focal adhesions of cells.[35] Here, we report for the first time a versatile and effective approach for the design of aligned electrospun CD nanofibers (CDNFs) functionalized with an adamantane-conjugated, laminin derived peptide epitope. In this system, the pentapeptide epitope Ile-Lys-Val-Ala-Val (IKVAV), a laminin derived sequence promoting neurite outgrowth,[36,37] was utilized as the bioactive cue. In this study, aligned cyclodextrin nanofibers (CDNFs) were produced in environmentally friendly conditions and functionalized with adamantane-conjugated IKVAV epitopes through host-guest interactions. Electrospinning of FDA approved modified CD[38,39] enabled us to obtain biocompatible high-aspect ratio CDNFs and a water-insoluble fibrous network with unique chemical and physical properties.[40] We observed that biofunctionalized aligned electrospun CDNFs direct the adhesion and neurite outgrowth of neuronal progenitor PC12 cells by providing a synergistic combination of physical and chemical cues.

Results and Discussion

Synthesis and Characterizations of IKVAV and KK peptides with random and aligned CDNFs

Adamantane (Ada), as a small guest hydrophobic molecule, is able to form a host-guest inclusion complex with CD due to its complementary size and high affinity to the hydrophobic CD cavity.[36,37] As shown in Figure 1, 1-adamantaneacetic acid units were covalently conjugated to two types of peptide backbones (either a

View Article Online
DOI: 10.1039/C6TB02441F

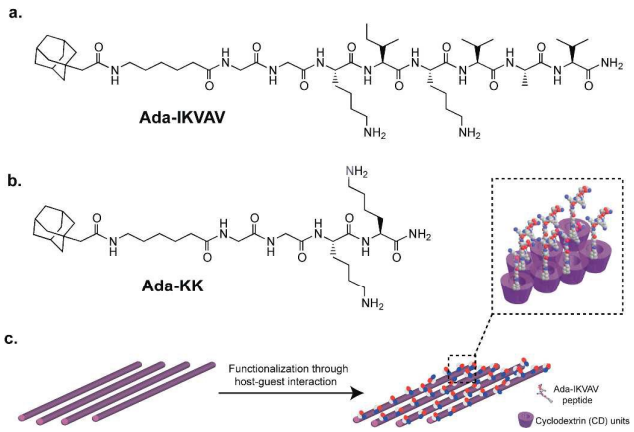

Figure 1. Chemical representation of a) Adamantane-6-aminohexanoic acid-GGKIKVAV-Am (IKVAV), b) Adamantane-6-aminohexanoic acid-GGKK-Am (KK). c) Schematic representation of electrospun and aligned CDNFs and host-guest interaction with bioactive peptide epitope.

control peptide (KK) or laminin mimetic epitope (IKVAV), which is known to induce the differentiation of neural progenitor cells into neurons, Figure 1a) using a 6-aminohexanoic acid molecule as a spacer (Figure 1b). The KK peptide consists of the same backbone with bioactive IKVAV peptide and has two positive charges at physiological conditions (Figure 1a, b). It was designed as an epitope-free control to examine the effects of the biochemical and biophysical cues on the neural differentiation capacity of the cells. Two glycine residues were conjugated between hydrophilic amino acid residues and the hydrophobic group to ensure that the bioactive cues are displayed at the surface. The peptide molecules were synthesized by using solid phase peptide synthesis method, purified with HPLC and characterized with LC-MS (Figure S1).

The functionalization of the polymer nanofiber surface was achieved through host-guest interactions following the incubation of electrospun CDNFs in peptide solutions (Figure 1c). Nile red assay[38] was used to determine the optimal peptide concentrations for minimizing aggregation and promoting the free integration of soluble peptide molecules into CD cavities. Critical aggregation concentrations (CAC) of IKVAV and KK peptides were determined as 60 µM and 125 µM, respectively (Figure S2). Therefore, CDNFs were incubated with 50 µM IKVAV and KK peptides for 24 h. The binding affinity of adamantane conjugated IKVAV and KK peptides to soluble CD was determined by ITC measurements (Figure S3). The inclusion complex was found to form at a 1:1 molar ratio. In addition, association constants of IKVAV and KK peptides were found as log Ka_{IKVAV}= 4.11 and log Ka_{KK} =4.08 respectively, which are comparable with association constants reported previously.[39] Structural properties of non-functionalized CDNFs and the peptide-functionalized materials were also analyzed with SEM (Figure 2). The images revealed that there is no significant difference between groups in terms of fiber diameter, which is close to 1 µm (Figure S4). Furthermore, noncovalent functionalization of CDNFs with peptide molecules did not cause any significant changes

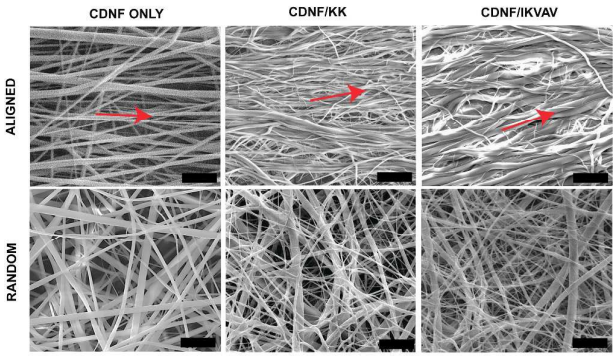

Figure 2. Scanning electron microscopy (SEM) images of random and aligned CDNFs with peptide functionalized forms (scale bars: 10 µm). Red arrow shows the alignment direction.

in the morphology of the CDNFs (Figure 2 and Figure S4). The presentation of peptide molecules on electrospun CDNFs through host-guest interactions was shown using a fluorescently labeled IKVAV peptide (FITC-IKVAV). After the incubation of both aligned and random CDNFs in peptide solution for 24 h, confocal images of the samples were acquired to monitor the distribution of the peptides on CDNFs. As shown in Figure 3, fluorescently labeled bioactive peptide molecules were homogenously distributed on both aligned and random electrospun CDNFs (Figure 3a).

In addition to fluorescence imaging, surface characterizations of the samples were also performed by XPS. Both random and aligned CDNFs showed only carbon and oxygen atoms (Figure S5a-d). On the other hand, functionalization of random and aligned CDNFs with KK and IKVAV peptides (Figure S5b-c) revealed an additional nitrogen peak indicating the existence of peptide layer on the surface (Figure 3c).

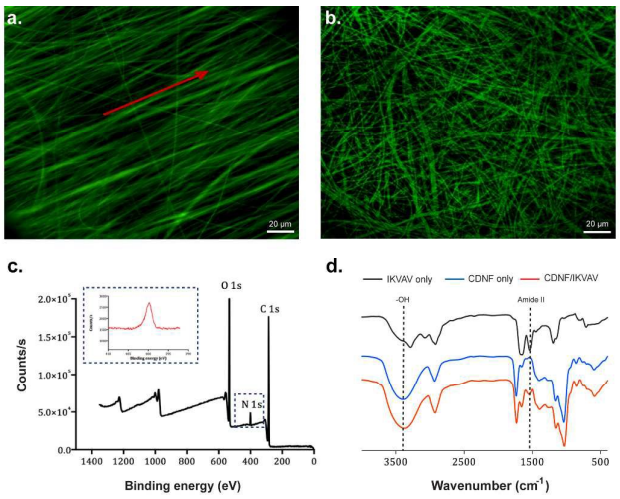

Figure 3. Aligned (a) and random (b) CDNFs functionalized with fluorescently labeled IKVAV. Red arrow shows the alignment direction **c.** XPS spectra of functionalized and aligned CDNFs. Inset shows the N1s (red line) peak and the presence of the peptide on the surface **d.** FTIR spectra of IKVAV, CDNFs and CDNFs/IKVAV.

View Article Online
DOI: 10.1039/C6TB02441F

To further investigate the formation of inclusion complexes between CDNFs and the peptide moieties, FT-IR spectra of the samples were obtained for both aligned and random morphologies (Figure 3d and Figure S6). In the case of bare CDNFs, a wide IR absorption band is present at 3390 cm^{-1} due to bending vibration of -OH group. However, peptide functionalization resulted in the red shift of the peak position from 3390 cm^{-1} to 3346 cm^{-1} due to the interactions between adamantane-peptide conjugates and the hydroxyl groups of CDNFs. In addition, the IR spectrum of the peptide-only group showed a typical amide II peak around 1533 cm^{-1} due to N-H bending.[40] A prominent amide II characteristic band is also present on the IR spectrum of peptide-functionalized CDNFs, further demonstrating the successful attachment of peptide molecules onto the electrospun fibers. Peptide content in this system was quantitatively determined by elemental analysis. The carbon, hydrogen, and nitrogen weight percentages within the samples are shown in Table S1. In contrast, nitrogen could not be detected on the random and aligned non-functionalized CDNFs due to the absence of peptide material. KK and IKVAV peptide amounts were calculated as 32.90% (w/w) and 30.62% (w/w) within random CDNFs; and 30.95% (w/w) and 30.81% (w/w) within the aligned CDNFs, respectively (Table S2).

Surface wettability is another important property for prospective biomaterials, as it is known to enhance cellular viability, adhesion and differentiation by effectively facilitating cell membrane-surface interactions.[41]Therefore, the surface hydrophilicity of both random and aligned CDNFs was investigated through contact angle measurements (Figure S7). Electrospun CDNFs with random and aligned fiber orientations were both strongly hydrophilic without requiring any additional treatments such as air plasma treatment, immobilization of proteins and chemical modifications. [42] Hence, the surface hydrophilicity of the electrospun CDNFs was found to be compatible with cellular interactions and can be used for cellular differentiation studies.

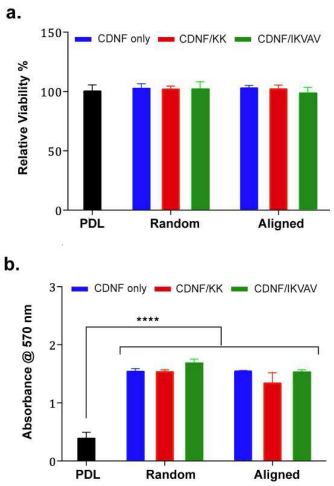

Figure 4. a) The relative viability of PC-12 cells cultured on random and aligned CDNFs, with or without peptide functionalization, compared to control group treated with poly-D-lysine (PDL) at 24 h b) Adhesion profiles of PC-12 cells after 2 h of incubation

Biocompatibility of electrospun CDNFs

The ability of electrospun CDNFs to induce neurite outgrowth and neural differentiation was evaluated using the PC-12 cell line, which differentiates into neural cells in the presence of soluble or substrate-derived physical and chemical factors. Figure 4 shows the biocompatibility and adhesion behaviors of the electrospun CDNFs under random and aligned fiber orientations and presenting either IKVAV or KK peptides. We observed that cellular viabilities on the scaffolds were comparable with poly-D-lysine (PDL) coated surfaces prepared as positive control (Figure 4a and Figure S8a), suggesting the materials are biocompatible.

Adhesion profiles of PC-12 cells cultured on CDNFs were also investigated, because differentiation of these cells requires their attachment to a substrate. Adhesion assay results revealed that electrospun CDNFs facilitated the attachment of PC-12 cells to a greater extent than PDL coated cover slips (Figure 4b and Figure S8b). The promoted cellular adhesion behavior on the scaffolds could be due to the affinity of cholesterol molecules located on the cell membrane to the hydrophobic cavity of CDNFs. [43,44]

Differentiation of PC-12 cells

Neural differentiation of PC-12 cells on CDNFs was studied by the immunostaining of the cells against synaptophysin I antibody, which is the most abundant protein at pre-synaptic axon terminals (Figure 5). [45] Synaptophysin expression was visualized to determine whether neurite outgrowth was enhanced on aligned CDNFs (Figure 5a). The role of CDNFs in directing neurite outgrowth was investigated by measuring the neurite lengths of PC-12 cells in order to gain quantitative information about neural differentiation.

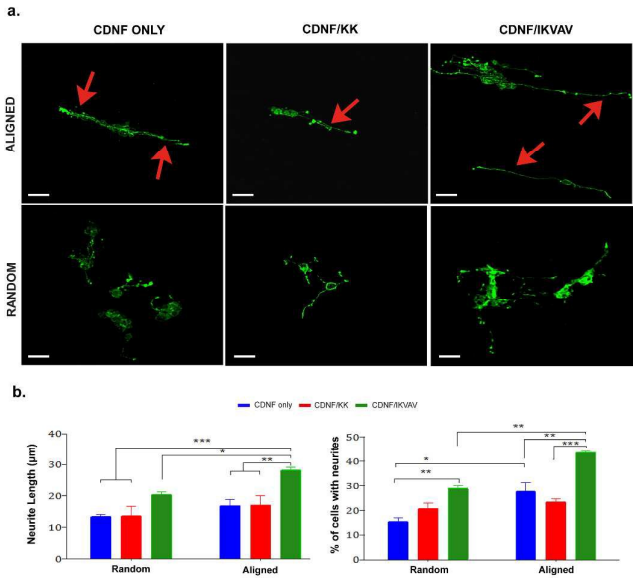

Figure 5. a) Synaptophysin expression of PC-12 cells cultured on random and aligned CDNFs with bioactive and non-bioactive functionalized peptide groups. Scale bars: 40 μm b) Neurite length and percentage of neurite bearing cells quantified by Image J at day 7 after induction reveals the aligned CDNFs functionalized with IKVAV is the most suitable scaffold for neurite outgrowth.

View Article Online
DOI: 10.1039/C6TB02441F

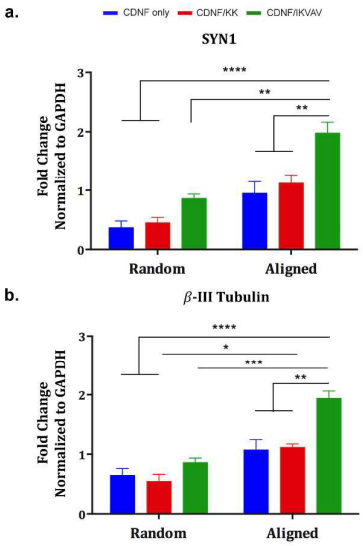

Figure 6. Expression of **a)** SYN1 and **b)** β-III tubulin normalized to control gene GAPDH. Values represent mean ± SEM (****p < 0.0001, ***p< 0.001, **p < 0.01, *p < 0.05).

Neurite extension lengths on aligned and IKVAV-functionalized CDNFs were nearly two times longer than non-functionalized and KK-functionalized random CDNFs (Figure 5b). Among the aligned CDNFs, IKVAV functionalized CDNFs induced significantly longer neurites, which underlines the importance of the bioactive epitope. In addition, the importance of fiber morphology was evident when the results were compared between random and aligned IKVAV-functionalized CDNFs (Figure 5b). Biofunctionalization and alignment also had a synergistic effect on the number of neurite-bearing cells (Figure 5b). Within each group the highest number of neurite-bearing cells was observed on the biofunctionalized scaffolds, while aligned CDNFs were found to further enhance this effect. These results suggest that both fiber alignment and biofunctionalization significantly promote the neural differentiation of PC-12 cells on electrospun scaffolds. The expression of the neural differentiation markers βIII-tubulin and SYN1 were also quantified at day 7 to determine the effect of biofunctionalized and aligned scaffolds on the genetic regulation of neurite extension. When PC-12 cells were cultured on the aligned CDNFs/IKVAV, the expression of the pre-synaptic axon terminal marker SYN1, was upregulated by ~5.5- and 4.4-fold compared to PC-12 cells cultured on random CDNFs only and CDNFs/KK surface, respectively (Figure 6a). In addition, the alignment of the fibers also had a significant effect on the upregulation of SYN1, as PC-12 cells on aligned CDNFs/IKVAV surfaces exhibit a 2.3-fold increase in SYN1 expression compared to the random CDNFs/IKVAV. In parallel with SYN1 expression, βIII-tubulin expression of cells cultured on aligned CDNFs/IKVAV scaffolds increased 3- and 3.6-fold compared to random CDNFs only group and CDNFs/KK, respectively (Figure 6b). Even in the absence of biofunctionality, a 2-fold increment difference was observed between random and aligned CDNFs/KK for βIII-tubulin expression, highlighting the importance of topological structure. Overall, we conclude that the neuroinductive effect of fiber alignment is more pronounced when biofunctional epitopes are presented at the surface of CDNFs.

Conclusions

Here we report the production of aligned CDNFs in environmentally friendly conditions and functionalization of these nanofibers with a laminin-derived epitope through host-guest chemistry for the enhancement of neural differentiation *in vitro*. The CDNFs/IKVAV hybrid system exhibited no toxicity to PC-12 cells, and provided an ideal environment for the induction of neuritogenesis through a combination of topographical and biochemical factors. The synergistic effect of biochemical and morphological cues facilitated the development of longer neurites than these obtained using only fiber alignment or bioactive signals for the induction of differentiation. In addition, we showed that neural differentiation was guided not only by the signals presented at the surface of CDNFs, but also through its interplay with the structural orientation of electrospun CDNFs. The biofunctionalized aligned CDNFs can be used as a potential material for nerve grafts and functional recovery in neural tissue engineering.

Experimental

Materials

All protected amino acids, Fmoc-6-aminohexanoic acid, Rink amide MBHA resin, 1-adamantaneaceticacid, fluorescein isothiocyanate isomer I (FITC), *N,N,N′,N′*-tetramethyl-O-(1*H*-benzotriazole-1-yl) uronium hexafluorophosphate (HBTU) and diisopropylethylamine (DIEA) were purchased from Novabiochem, ABCR or Sigma-Aldrich. The hydroxypropyl-β-cyclodextrin (HPβCD) (degree of substitution: ~0.6, Cavasol®W7 HP Pharma) was kindly donated by Wacker Chemie AG (Germany). 1,2,3,4-butanetetracarboxylic acid (BTCA, 99%) and sodium hypophosphite hydrate were commercially obtained from Sigma-Aldrich. All other chemicals and materials used in this study were analytical grade and purchased from Invitrogen, Fisher, Merck, Alfa Aesar, and/or Sigma-Aldrich.

Synthesis and Characterization of Peptides

Fmoc solid phase peptide synthesis method was used in order to synthesize adamantane-6-aminohexanoicacid-Gly-Gly-Lys-Ile-Lys-Val-Ala-Val-Am (IKVAV), adamantane-6-aminohexanoicacid-Gly-Gly-Lys-Lys-Am (KK) and adamantane-6-aminohexanoicacid-Gly-Gly-Lys-Lys(FITC)-Ile-Lys-Val-Ala-Val-Am (FITC-IKVAV). Rink amide MBHA resin (Novabiochem) served as a solid support for the synthesis all peptide molecules. In order to activate carboxylate groups. 2 moles equivalents of amino acid, 3 moles equivalents of diisopropylethylamine (DIEA) and 1.95 mole equivalents of *N,N,N′,N′*-tetramethyl-O-(1*H*-benzotriazole-1-yl) uronium hexafluorophosphate (HBTU) were used for 1 mole equivalent of solid resin. For each coupling step, 10% acetic anhydride-DMF solution was used to acetylate the unreacted amine groups and Fmoc protecting groups were removed with 20% piperidine/dimethylformamide (DMF) for 20 min. The coupling time for the amino acids and Fmoc-6-aminohexanoic acid was 2 h for each cycle. The coupling mechanism of 1-adamantaneacetic acid was similar to the amino acid coupling steps. Between each of these steps, resins were washed three times using DMF, DCM and DMF, respectively. For FITC conjugation to IKVAV peptide, 4- methyltrityl (Mtt) protecting group of –Lys was removed using 60 mL cleavage

View Article Online
DOI: 10.1039/C6TB02441F

solution containing 2.85 mL TFA, 0.075 mL distilled water, 0.075 mL triisopropylsilane and 57 mL DCM. The resins were shaken with 10 mL of this solution 6 times for 5 min each, then washed with DCM until the yellow color in the washing DCM had disappeared. Finally, the resins were washed with 5% (v/v) DIEA in DCM prior to FITC coupling. The FITC coupling solution containing 389.4 mg FITC and 256.8 µL DIEA was prepared in 3 mL DMF and added on the resins. The reaction vessel was covered with aluminum folio in order to prevent the bleaching of FITC. For scaffold functionalization studies, FITC was combined with IKVAV at a ratio of 5 mol %. After the completion of the synthesis, peptides were cleaved from the solid supports with a solution of 95% trifluoroacetic acid (TFA), 2.5% distilled water, and 2.5% triisopropylsilane. The cleavage reaction was continued for 3 h by shaking the resins with the cleavage solution. Then, the resins were washed with DCM to collect the cleaved peptides into the flask. Excess TFA and DCM were removed by rotary evaporator, and peptides were precipitated in ice-cold diethyl ether overnight. To remove ether, centrifugation was performed at 8000 rpm for 20 min. The precipitated peptides were dissolved in distilled water and kept at -80 °C overnight. The lyophilization of the frozen peptide solutions was carried out for 3 days in order to obtain dried peptide powders. The purity of the peptides was determined by Agilent 6530 quadruple time of flight (Q-TOF) mass spectrometry with an electrospray ionization (ESI) source. Further purification was performed with a preparative HPLC system (Agilent 1200 series).

Electrospinning of cyclodextrin nanofibers (CDNFs)

Crosslinked water-insoluble CDNF was obtained by electrospinning an aqueous HPβCD solution and BTCA was used as a cross-linker. The electrospinning parameters were adjusted as follows; 0.5-2 mL/h flow rate, 10-20 kV applied voltage and 10-20 cm collector distance. Randomly oriented CDNF were deposited on a grounded fixed metal collector, while a rotating drum at a speed of 2000 rpm was used to obtain aligned CDNFs.

Critical Aggregation Concentration (CAC) determination

A hydrophobic nile red (9-diethylamino-5-benzo[α]phenoxazinone) fluorescent probe assay was used to determine the transition phase between peptide assemblies and facilitate greater control over scaffold morphology. Peptide solutions (ranging from 1 mM to 0.244 µM) were prepared in distilled water at around pH 7, while 1.25 mM stock solution of Nile red was prepared in ethanol (1 mL) and then diluted to 78.12 µM by using ethanol. Peptide solutions prepared at different concentrations were mixed with the same amount of the dye solution; and incubated overnight at room temperature. Final Nile red concentration in the mixtures was 250 nM; and 0.31% (v/v) ethanol was present in the solutions. A Cary Eclipse Spectrophotometer was used to collect emission spectra between 580 nm and 750 nm with an excitation of 550 nm.

Functionalization of CDNFs with peptides

Electrospun CDNFs were washed with ethanol and water, immersed in the peptide solutions (IKVAV or KK) and incubated for 24 h in order to functionalize CDNF surfaces with peptide molecules through host-guest interactions at a 1:1 molar ratio.

Scanning Electron Microscopy (SEM)

Morphologies of CDNFs and peptide-functionalized CDNFs were analyzed with a FEI Quanta 200 FEG scanning electron microscope. All samples were coated with 8 nm Au–Pt prior to imaging and the analysis was performed at 15 kV. The diameters of electrospun fibers were quantified by ImageJ software by measuring the diameters of 30 x 8 nanofibers from eight different SEM images.

X-ray photoelectron spectroscopy (XPS)

XPS analyses of samples were conducted by using a Thermo K-alpha monochromated high performance X-ray photoelectron spectrometer. CDNFs and peptide-immobilized systems were analyzed after washing. Survey analyses were performed at 3 scans. High-resolution spectra for carbon and oxygen were recorded at 10 scans while nitrogen was scanned at 15 scans.

FT-IR spectroscopy

A Fourier Transform Infrared Spectrometer (FT-IR) (Bruker-Tensor 37) was used for the collection of IR spectra of the samples. Non-functionalized and peptide functionalized CDNFs prepared at both aligned and random electrospun fiber organizations were mixed with potassium bromide (KBr) to prepare the pellets by pressing. The IR spectra were recorded between 4000 and 400 cm^{-1} at a resolution of 4 cm^{-1} with 64 scans recorded for each sample.

Elemental Analysis

After host-guest functionalization, peptide contents in electrospun CDNFs were analyzed using a Thermo Scientific FLASH 2000 series CHNS-O analyzer. Both random and aligned CDNFs and their peptide-functionalized forms were analyzed. As a standard, 2,5-(bis(5-*tert*-butyl-2-benzo-oxazol-2-yl)) thiophene was used as a standard. For each analysis, vanadium pentoxide was used as a catalyst for complete oxidation.

Isothermal Titration Calorimetry

Stoichiometry and association constants between CD units and guest peptides (IKVAV and KK) were determined using ITC (Microcal ITC200). 40 µL of 5 mM CD solution was injected in 1.5 µL increments to cells containing 280 µL 350 µM IKVAV or 700 µM KK solutions. During the measurements, the cell temperature was 25 ºC, reference power was 3.5 mcal s^{-1}, and stirring speed was 1000 rpm.

Contact Angle Measurements

The wettability of electrospun CDNFs was measured using an optical contact angle measurement system (Dataphysis OCA30). Ultra-pure water was used as the testing liquid.

Fluorescent Imaging

The functionalization of CDNFs with the peptide molecules through host-guest interactions were also analyzed by incubating FITC conjugated IKVAV peptide with the electrospun CDNFs overnight. Electrospun CDNFs were washed with ethanol and water prior to the imaging. The fluorescence images were acquired using a Zeiss LSM510 microscope under 20X magnification. Peptide solutions used for the fluorescent imaging were prepared by mixing FITC-IKVAV with non-labeled IKVAV peptide at a 1:19 molar ratio, respectively.

Cell Viability and Adhesion Assays

PC-12 cellular viability and adhesion analyses were performed in a 48-well plate. Before cell culture experiments, 9 mm cover slips

View Article Online
DOI: 10.1039/C6TB02441F

coated with parafilm were immersed in 96% (v/v) ethanol solution for 30 min and sterilized with UV for 15 min. Coverslip-sized electrospun nanofiber mats were cut and treated with 70% (v/v) ethanol for 30 min for sterilization. Then, the scaffolds were exposed to cell culture medium at 37 °C for 6 h. PC-12 cells ($5.0x10^4$ per well) were seeded on the electrospun scaffolds containing Roswell Park Memorial Institute medium (RPMI) with 10% horse serum (HS), 5% fetal bovine serum (FBS), 2 mM L-glutamine and 1% penicillin/streptomycin (P/S), and incubated at 37°C in 5% (v/v) CO_2 for 24 h and 48 h. MTT (3-(4,5-dimethylthiazol-2-yl)-2,5-diphenyltetrazolium bromide) method was used to evaluate the activity of cells on the electrospun fibers. 270 µL of DMEM (Dulbecco's Modified Eagle Medium) without phenol red and 30 µL of MTT was added into each well and cultivated for 4 h under standard cell culture conditions. All nutrient solution was removed, and 300 µL of MTT solubilization solution was added into each well and pipetted at constant temperature in order to dissolve the crystals. The purple solution was transferred into a 96-well culture plate (200 µL/well), and its absorbance was measured at 570 nm using a micro plate reader (M5, Molecular Devices) The cell adhesion assay was performed as previously described.[46] Briefly, the cells were incubated with 4 mg/mL BSA and 50 µg/mL cyclohexamide in serum-free medium for 2 h and 4 h at 37 °C with 5% CO_2. Then, 500 µL of PC-12 cells ($1 x 10^5$ cells/mL) were seeded with medium containing 4 mg/mL BSA and 50 µg/mL cyclohexamide for 2 h. After the incubation, unattached cells were washed with PBS twice. The attached cells were fixed with 4% formaldehyde in PBS for 15 min and then stained with 0.5% crystal violet for 1 h. After that point, experiment was conducted under dark conditions. The plates were gently washed with distilled water five times and cellular membranes were distrupted with 2% SDS for 10 min. Absorbance was measured at 570 nm with a M5 microplate reader.

Immunocytochemistry (ICC)

Prior to neural induction, PC-12 cells ($5 x 10^4$ per well) were cultured on the materials for 24 h at standard cell culture conditions. Then the medium was replaced with freshly prepared neural induction medium containing MEM with 2% HS, 1% FBS, 2 mM L-glutamine and 1% P/S and 20 ng/mL NGF. The cells were cultured on the materials for seven days and fixed with 500 µL/well pre-warmed 4% paraformaldehyde/PBS for 15 min at room temperature. After discarding paraformaldehyde, the cells were washed with 0.3% triton-X100/PBS for 15 min at room temperature on a shaker. Then, blocking was carried out with 10% normal goat serum (NGS) and 1% bovine serum albumin (BSA) in PBS with 0.3% Triton-X for 1 h at room temperature on a shaker. After aspirating the blocking solution, the cells were treated with primary antibodies against Synaptophysin at 1: 400 dilution. The cell culture plates were sealed with parafilm and incubated overnight at 4 °C on a nutator shaker. On the next day, the plates were incubated for 1 h at room temperature. Then, cells were washed with 0.3% PBS/Triton- X100 for 5 min and twice with PBS for 5 min on rocking shaker. After this point, the experiment was continued under darkness. A secondary antibody (GAR AF488) in 10% BSA was added to the wells and incubated for 1 h. Washing steps were again performed with PBS and finally distilled water on the shaker. A drop of Prolong Gold Mounting Medium was added onto the slides of each coverslip. The coverslips were then taken out from each well, inverted and exposed to a mounting solution on slides. 8 images were taken from each well with a Zeiss LSM510 confocal microscope under 20x magnification. Neurite extensions were quantified by Image J, and average neurite length was obtained from three independent replicates.

Quantitative Reverse Transcription Polymerase Chain Reaction (qRT-PCR)

Synaptophysin and βIII-tubulin gene expression profiles were examined by qRT-PCR. Total RNA of the differentiated PC-12 cells was isolated on day 7 using TRIzol reagent (Invitrogen) according to the manufacturer's protocol. The yield and purity of the isolated RNA were quantified by Nanodrop 2000 (Thermo Scientific). Primer sequences were designed using NCBI database (Table S3). SuperScript III Platinum SYBR Green one-step qRT-PCR kit was used to conduct qRT-PCR. Temperature cycling for the reaction was determined as 50 °C for 3 min, 95 °C for 5 min, 40 cycles of 95 °C for 15 s, T_m (58.0 °C for Synaptophysin and βIII-tubulin) for 30 s, and 40 °C for 1 min, respectively. Amplification was analyzed by determining the binding of SYBR I to double stranded DNA. Gene expressions were normalized to GAPDH as the internal control gene.

Statistical Analysis

All experiments were independently repeated at least twice with at least three replicates for each experimental group. All quantitative results were expressed as ± standard error of means (sem). Statistical analyses were carried out by one-way or two-way analysis of variance (ANOVA), whichever applicable.

Acknowledgements

This work was partially supported by the Scientific and Technological Research Council of Turkey (TUBITAK) and Turkish National Academy of Sciences (TUBA). We thank Melike Sever and Gokhan Gunay for helpful scientific discussions and gene expression analysis. We also thank Zeynep Erdogan's help for ITC and LC-MS.

Notes and references

* Corresponding authors and contact information; e-mails:
moguler@unam.bilkent.edu.tr (M.O.G.) and
atekinay@unam.bilkent.edu.tr (A.B.T.) and
uyar@unam.bilkent.edu.tr (T.U.)

1 Thuret, S.; Moon, L. D. F.; Gage, F. H. *Nat. Rev. Neurosci.* **2006**, 7, 628.
2 De Luca, A. C.; Lacour, S. P.; Raffoul, W.; di Summa, P. G. *Neural Regen. Res.* **2014**, 9, 1943.
3 Gu, X.; Ding, F.; Yang, Y.; Liu, J. *Prog. Neurobiol.* **2011**, 93, 204.
4 Kelleher, C. M.; Vacanti, J. P. *J. R. Soc. Interface* **2010**, 7, 717–729.
5 Ingber, D. E.; Mow, V. C.; Butler, D.; Niklason, L.; Huard, J.;

View Article Online
DOI: 10.1039/C6TB02441F

Mao, J.; Yannas, I.; Kaplan, D.; Vunjak-Novakovic, G. *Tissue Eng.* **2006**, 12, 3265.
6 Mammadov, B.; Sever, M.; Guler, M. O.; Tekinay, A. B. *Biomater. Sci.* **2013**, 1, 1119.
7 Bellamkonda, R. *Biomaterials* **2006**, 27, 3515.
8 Frantz, C.; Stewart, K. M.; Weaver, V. M. *J. Cell Sci.* **2010**, 123, 4195.
9 Gardiner, N. J. *Dev. Neurobiol.* **2011**, 71, 1054.
10 Ramakrishna, Seeram, Fujihara K. *World Scientific.* **2005**, 342.
11 Greiner, A.; Wendorff, J. H. *Angew. Chem.* **2007**, 46, 5670.
12 Garifullin, R.; Ustahuseyin, O.; Celebioglu, A.; Cinar, G.; Uyar, T.; Guler, M. O. *RSC Adv*. **2013**, 3, 24215.
13 Agarwal, S.; Wendorff, J. H.; Greiner, A. *Polymer.* **2008**, 49, 5603.
14 Cunha, C.; Panseri, S.; Antonini, S. *Nanomedicine Nanotechnology, Biol. Med.* **2011**, 7, 50.
15 Liang, D.; Hsiao, B. S.; Chu, B. *Adv. Drug Deliv. Rev.* **2007**, 59, 1392.
16 Ni, H. C.; Lin, Z. Y.; Hsu, S. H.; Chiu, I. M. *Acta Biomater.* **2010**, 6, 2066.
17 Yoo, H. S.; Kim, T. G.; Park, T. G. *Adv. Drug Deliv. Rev.* **2009**, 61, 1033.
18 Yao, L.; Wang, S.; Cui, W.; Sherlock, R.; O'Connell, C.; Damodaran, G.; Gorman, A.; Windebank, A.; Pandit, A. *Acta Biomater.* **2009**, 5, 580.
19 Smith Callahan, L. a.; Xie, S.; Barker, I. a.; Zheng, J.; Reneker, D. H.; Dove, A. P.; Becker, M. L. *Biomaterials* **2013**, 34, 9089.
20 Koh, H. S.; Yong, T.; Chan, C. K.; Ramakrishna, S. *Biomaterials* **2008**, 29, 3574.
21 Park, H.; Lee, J. W.; Park, K. E.; Park, W. H.; Lee, K. Y. *Colloids Surfaces B Biointerfaces* **2010**, 77, 90.
22 Zhao, W.; Li, J.; Jin, K.; Liu, W.; Qiu, X.; Li, C. *Mater. Sci. Eng. C* **2016**, 59, 1181.
23 Kijenska, E.; Prabhakaran, M. P.; Swieszkowski, W.; Kurzydlowski, K. J.; Ramakrishna, S. *Eur. Polym. J.* **2014**, 50, 30.
24 Bini, T. . B.; Gao, S.; Wang, S.; Ramakrishna, S. *J. Mater. Sci.* **2006**, 41, 6453.
25 Xie, J.; Liu, W.; Macewan, M. R.; Bridgman, P. C.; Xia, Y. *ACS Nano* **2015**, 8*,* 1878.
26 Kim, Y.; Haftel, V. K.; Kumar, S.; Bellamkonda, R. V. *Biomaterials* **2008**, 29, 3117.
27 Hurtado, A.; Cregg, J. M.; Wang, H. B.; Wendell, D. F.; Oudega, M.; Gilbert, R. J.; McDonald, J. W. *Biomaterials* **2011**, 32, 6068.
28 Wang, H. B.; Mullins, M. E.; Cregg, J. M.; Hurtado, A.; Oudega, M.; Trombley, M. T.; Gilbert, R. J. *J. Neural Eng.* **2009**, 6, 16.
29 Schmidt, B. V. K. J.; Hetzer, M.; Ritter, H.; Barner-Kowollik, C. *Prog. Polym. Sci.* **2014**, 39, 235.
30 Celebioglu, A.; Uyar, T. *Chem. Commun.* **2010**, 46, 6903.
31 Stoffelen, C.; Huskens, J. *Small* **2016**, 12, 96.
32 Hu, Q.; Tang, G.; Chu, P. K. *Acc. Chem. Res.* **2014**, 47, 2017.
33 Boekhoven, J.; Rubertpérez, C. M.; Sur, S.; Worthy, A.; Stupp, S. I. *Angew. Chemie.* **2013**, 52, 12077.
34 Mammadov, B.; Mammadov, R.; Guler, M. O.; Tekinay, A. B. *Acta Biomater.* **2012**, 8, 2077.
35 Silva, G. A.; Czeisler, C.; Niece, K. L.; Beniash, E.; Harrington, D. A.; Kessler, J. A.; Stupp, S. I. *Science* **2004**, 303, 1352.
36 Paolino, M.; Ennen, F.; Lamponi, S.; Cernescu, M.; Voit, B.; Cappelli, A.; Appelhans, D.; Komber, H. *Macromolecules* **2013**, 46, 3215.
37 Rodell, C. B.; Mealy, J. E.; Burdick, J. A. *Bioconjug. Chem.* **2015**, 26, 2279.
38 Kurniasih, I. N.; Liang, H.; Mohr, P. C.; Khot, G.; Rabe, J. P.; Mohr, A. *Langmuir* **2015**, 31, 2639.
39 Eftink, M. R.; Andy, M. L.; Bystrom, K.; Perlmutter, H. D.; Kristol, D. S. *J. Am. Chem. Soc.* **1989**, 111, 6765.
40 Paramonov, S. E.; Jun, H.; Hartgerink, J. D. *J. Am. Chem. Soc.* **2006**, 128, 7291.
41 Martins, A.; Pinho, E. D.; Faria, S.; Pashkuleva, I.; Marques, A. P.; Reis, R. L.; Neves, N. M. *Small* **2009**, 5, 1195.
42 Ma, Z.; Mao, Z.; Gao, C. *Colloids Surfaces B Biointerfaces* **2007**, 60, 137.
43 Tsamaloukas, A.; Szadkowska, H.; Slotte, P. J.; Heerklotz, H. *Biophys. J.* **2005**, 89, 1109.
44 López, C. A.; de Vries, A. H.; Marrink, S. J. *Sci. Rep.* **2013**, 3, 1.
45 Kwon, S. E.; Chapman, E. R. *Neuron* **2011**, 70, 847.
46 Jung, S. Y.; Kim, J. M.; Min, S. K.; Kim, O. B.; Jang, D. H.; Kang, H. K.; Min, B. M. *Biomaterials* **2012**, 33, 3967.

View Article Online
DOI: 10.1039/C6TB02441F

Table of Content Image

Noncovalent functionalization of electrospun cyclodextrin nanofibers (CDNFs) via bioactive peptide epitope through host-guest interactions is presented to develop functional scaffolds for nerve cell engineering; and the synergistic combination of the biochemical and biophysical cues results the enhanced neural outgrowth and neural differentiation on the scaffolds.